Fabrication of 3D Screen-Printed Micro-Cavities Towards Sweat Sensors for Integrated Flexible Hybrid Electronics

Cameron Anderson¹, Z. Hugh Fan², Jorg Richstein³, Mark Sussman³, Toshikazu Nishida¹

¹Dept. of Electrical and Computer Engineering, University of Florida, Gainesville, USA

²Dept. of Mechanical Engineering, University of Florida, Gainesville, USA

³Jabil, St. Petersburg, FL, USA

nishida@ufl.edu

Abstract— Cavities fabricated on the microscale have a wide variety of applications, from microwells for cell cultures, microfluidic channels for drug delivery systems to waveguide structures for RF applications. Microcavities are particularly useful for sensing applications, such as cavity-based pressure sensors and gap-based capacitive sensors. Cavity structures have been widely demonstrated in MEMS devices using typical semiconductor processing. However, the development of similar structures for flexible applications poses additional challenges. While flexible cavity structures have been fabricated in laboratory environments, challenges arise when these structures are integrated into a larger flexible sensing device or flexible hybrid electronics system. An additive manufacturing approach to cavity formation is presented which utilizes a 3D screen-printing process and in-situ cure. Patterned microstructures are formed by building up layers of dielectric ink interspersed as needed with printed conductive traces. A proof-of-concept microfluidic channel-based capacitor is fabricated to demonstrate the potential sensing applications for the fabricated microcavities.

Keywords—flexible sensing; micro-cavities; screen-printing; printed electronics

I. INTRODUCTION

Microcavities have become a prominent component of research in many fields, with applications from engineering to biology. Optical microcavities, which confine light in small volumes using resonance, are a prominent field of research with applications from quantum optics to bio and chemical sensing [1]. In the field of biomedical research, microcavity arrays have been widely used for cell isolation and analysis, and micro-needles have been developed for drug delivery systems [2], [3], [4], [5]. Microfluidic channels enable lab-on-a-chip applications such as cell culture, disease diagnosis, and tissue-on-chip devices. Additionally, MEMS transducers rely heavily on fabricated microcavities, and have been shown to be particularly effective for a wide range of sensing applications, such as pressure transducers, gyroscopes, and accelerometers [6], [7], [8]. MEMS devices are typically fabricated through surface or micromachining, utilizing photolithographic patterning and etching processes on common semiconductor substrates such as Si or Ge.

This research was supported in part by the National Science Foundation I/UCRC on Multi-functional Integrated System Technology (MIST) Center IIP-1939009.

Flexible sensing has emerged as a prominent field in recent years as the demand for wearable biosensors has grown [9]. However, traditional subtractive manufacturing techniques pose a challenge for the development of flexible sensors, due to material compatibility and temperature constraints. As such, new methods for the development and integration of microstructures commonly used in MEMS sensors are necessary to develop flexible biosensors, and to successfully integrate these devices into broader flexible electronic systems.

Additive manufacturing techniques such as inkjet and 3D printing have grown in popularity for the development of flexible electronics due to their rapid prototyping capabilities [9]. These methods are primarily utilized for the fabrication of conductive traces and electrodes, which are then combined with other fabrication techniques such as laser etching or soft lithography to create a flexible sensor [10], [11], [12]. Each additional fabrication technique utilized in a device design increases manufacturing complexity and cost, which limits scalability of these techniques to low-cost, highvolume manufacturing. 3D screen printing, the process of building up three dimensional structures through successive screen-printed layers, offers a unique approach to the lowcost fabrication of flexible microcavities [13]. Few examples of this approach have been demonstrated for flexible electronics, but the technique allows for design flexibility to create devices which can be directly integrated into a flexible hybrid electronics manufacturing process, reducing manufacturing complexity [13], while delivering fully flexible integrated systems.

Here, we present a 3D screen printed and in situ curing approach to flexible microcavity fabrication for flexible hybrid electronics applications. The fabrication process is compatible with a variety of commercially available flexible inks and can be used to print complex geometric microcavity structures directly integrated with electronic interconnects and processing circuitry. A flexible microfluidic channel was fabricated and tested as a capacitive sensor towards sweat sensing as part of an integrated sensing platform as a proof of concept.

II. MATERIALS AND METHODS

A. Materials

The ink chosen for this work was DI-7548 (Nagase ChemTex), an isobornyl acrylate-based resin ink which is

UV curable using a mercury vapor lamp. This ink is commonly used as an encapsulant for printed Ag traces to prevent oxidation, and to create trace crossover areas in printed electronic circuits. Other commercial inks are available as UV cured or thermally cured, and are made from a variety of materials, such as acrylate resin, epoxy, and silicone, and can be chosen based on the needs of the designed devices. Stainless steel mesh screens were manufactured by Microscreen, LLC. Curing methods using UV LEDs were investigated to improve the compatibility of the process with available equipment as well as to mitigate print registration errors. Structures were printed using a DEK Horizon 03i automatic screen printer modified to facilitate in situ curing of dielectric ink layers.

B. Cavity Fabrication

Flexible cavities were fabricated using a 3D screen printing method consisting of successive printing of dielectric layers, as shown in Fig. 1. Substrates of 7-mil-thick polyethelene terepthalate (PET) were prepared by cleaning the surface with 99% isopropyl alcohol (Fisher Chemical) to remove any environmental contaminants. A graphic layer was screen printed to create fiducials, and additional markings for the specific device fabrication. Final substrate preparation, including the cutting of vias and screen printing of conductive traces was then completed. The first dielectric ink layer was deposited using a stainless-steel mesh screen patterned with the cavity geometry (Step 4), cured using UV LEDs, then repeated until the desired cavity height was reached (Steps 5-7). A laminated roller press adhered a thermal film to the top of the patterned (Step 8). Additional device elements were screen printed on top of the film to complete the devices.

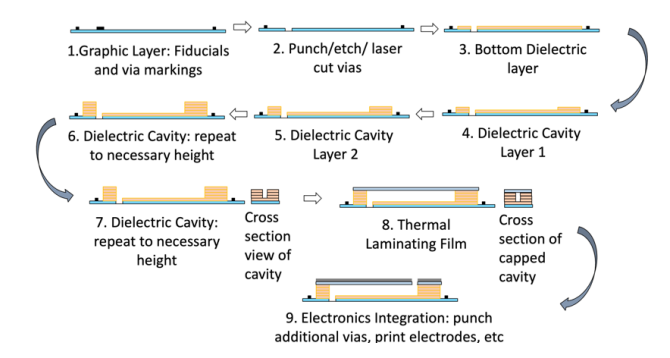


Fig. 1. Fabrication process flow of 3D screen-printed flexible microcavities. Successive layers of dielectric ink are printed and cured until the desired height is reached.

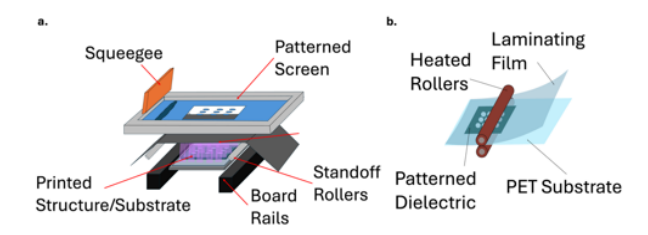


Fig. 2. a. Diagram of the designed in situ curing system. A retractable sheet with flexible UV LEDs is extended between the screen and substrate during curing. b. Illustration of the lamination process to cap the fabricated cavities.

C. In Situ Cure

To reduce the potential for registration errors between layers of the printed channel, an in-situ UV curing system was developed which can be mounted onto the commercial screen printer. Fig. 2a shows a diagram of the designed setup, consisting of a retractable, flexible UV blocking vinyl sheet with adhered UV LEDs which extend between the substrate and the screen after printing a layer of dielectric ink. The sheet is supported by a system of detachable standoffs and rollers and is retracted away from the printing area when not in use. LEDs of multiple wavelengths (365 nm, 395 nm) to simulate the broad-spectrum mercury vapor lamp LED systems more closely are used. The retractable nature of the setup allows for the substrate to remain in the same place during curing, reducing the potential for registration errors or other defects to occur during the curing process.

D. Capping

A thermal laminating film made of PET (GBC, Acco Brands LLC) was used for capping the printed cavities. PET was selected to ensure compatibility between the selected inks and the capping layer, as well as for its low processing temperature. The thermal film was aligned on top of the completed trenches and passed through a laminating machine at 105°C (Fig. 2b.). The combined heat and pressure activate the adhesive to ensure complete bonding between the laminating film and the printed devices. Due to the aspect ratio of the printed structures, the film adheres only to the printed dielectric ink which forms the cavity walls, leaving an open cavity of the designed geometry. This approach is a low cost, easy to manufacture method of cavity capping which can be incorporated into batch fabrication or roll-toroll printing processes which enables screen printing of additional layers after capping. This allows for flexibility in the design of complex geometric cavities which may incorporate internal membrane structures and conductive interconnects.

III. DISCUSSION

Characterization of the printed microcavity was performed to analyze the structure's geometry and the impact of print parameters on the final structure. Fig. 3 shows an example of a screen printed microfluidic channel structure. Evaluation of the measured cavity width in relation to the designed geometry and height as a function of deposited layers was performed using stylus profilometry (Dektak 150, Tencor Alpha-step AS500), as shown in Fig. 4. Fig. 4a shows linear growth in height, indicating that the thickness of the



Fig. 3. Printed microfluidic channel test structure using the described flexible cavity fabrication process. The printed structure has been capped with a laminating film and inlet and outlet holes have been punched in the capping layer to allow fluid flow. The cavity has been filled with dyed water to illustrate its functionality as a microfluidic channel.

deposited layers is not affected by the height of the structure. The calculated thickness per layer is 12.7 $\mu m.$

Fig. 4b shows the reduction of cavity width as a function of layers for the particular ink and curing conditions used in this test. The difference in the measured width of the channel compared to the designed width is due to ink bleed during the printing process, and can vary based on the specific printing parameters and ink chosen. The minimum width achieved under these conditions was 30 μm using a 100 μm designed width and 1 print layer. At a designed width of 200 μm , measured widths of $\sim \! 100 \mu m$ were achieved up to 14 print layers. Fig. 4c illustrates the measurement points for all indicated cavity measurements.

Computed tomography images (Zeiss Versa 620) were taken to analyze the 3D structure and calculate cross-sectional areas. Fig. 5a shows a decrease in channel width from ${\sim}920~\mu m$ to ${\sim}726~\mu m$ when printing parallel vs. perpendicular to the print direction. Fig. 5b shows that the sidewalls formed at an angle of 53°, likely due to the ink bleed of each successive layer flowing towards the substrate before curing.

A 1 mm designed width microfluidic capacitive test structure was fabricated as a proof of concept for flexible sweat sensing. The approximate channel volume was calculated as $2.7~\mu L$. The test setup uses a syringe pump for precise dispensing of water through a NanoPort connector, and an impedance analyzer to measure capacitance (HP 4914A). Preliminary tests demonstrate measurable capacitance changes from 3 pf to 7 pF as fluid volume

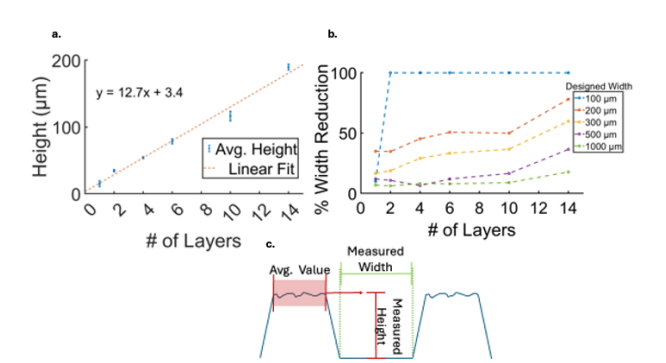


Fig. 4. a. Measured height of fabricated cavity structures as a function of the number of deposited layers demonstrates linear growth. b. Measurement of percent reduction of width for each designed cavity width. c. Illustration of measurement locations.

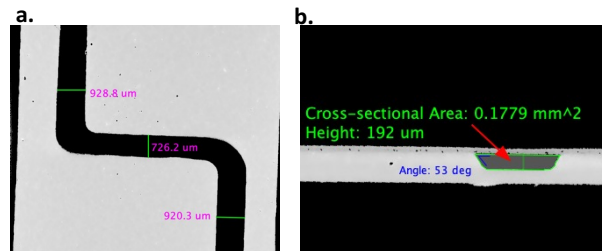


Fig. 5. a. Mid-plane cross-section image of the fabricated structure shows variation in fabricated channel width between print orientations for a single device. b. Perpendicular cross-section image of the fabricated device. Measured cross-sectional area is 0.1179 mm², with a measured cavity height of 192 um.

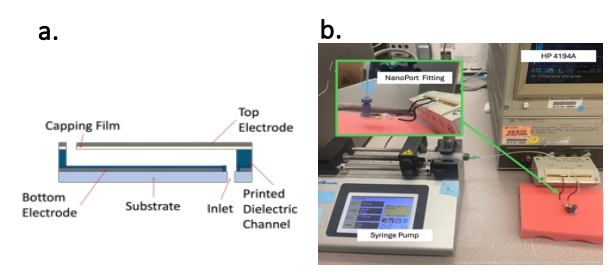


Fig. 6. a. Cross section diagram of the fabricated capacitive sensor. Test setup of the microfluidic capacitance sensor includes a syrir pump to control fluid flow, a NanoPort fitting on the sample inlet, and impedance analyzer (HP 4194A).

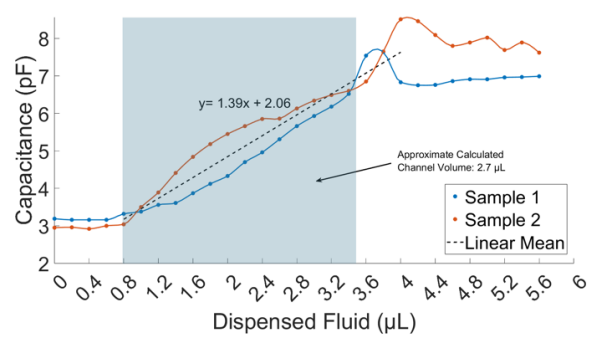


Fig. 7. Measured capacitance of microfluidic channel samples. Capacitance rose from 3 pF to 7 pF in the region of channel filling (blue region). A linear fit of the mean shows an approximate sensitivity of 1.39 pF/ μ L.

increases up to the calculated channel volume (Fig. 7), with an average capacitance of 1.39 pF/ μ L for the samples tested. Additional investigation and modelling of fluid flow within the inlet and channel is needed to understand the observed exit effect on capacitance as well as to characterize the filling behavior of the channel. Additionally, exploration of optimal device design for sweat sensing including duration of use and bending strain compensation will be pursued in future work.

IV. CONCLUSIONS

3D screen printing and in situ curing has been demonstrated to successfully create microcavities on flexible substrates. A proof-of-concept microfluidic channel-based capacitor was fabricated to demonstrate sensing of fluid volume. These structures show promise for the fabrication of directly integrated flexible biosensors for wearable sensing systems, from membrane-based pressure sensors to small sample fluid collection and analysis, and optical microcavity based sensors. Characterization of the effects of geometry design and print orientation show that the effect of print bleed needs to be accounted for in the device design to ensure final devices meet the desired specifications. The screenprinted approach offers significant flexibility for design and integration with broader printed flexible electronics, and reduces fabrication complexity, broadening the potential to develop low-cost flexible integrated sensing systems for wearable devices.

Future work will investigate the application of this fabrication method to the design and characterization of a flexible sweat rate sensor based on capacitive transduction which will be incorporated into a broader multi-functional wearable sensing system.

REFERENCES

- [1] H. Megahd, D. Comoretto, and P. Lova, "Planar microcavities: Materials and processing for light control," *Optical Materials: X*, vol. 13. Elsevier B.V., Jan. 01, 2022.
- [2] M. Hosokawa et al., "Size-Based Isolation of Circulating Tumor Cells in Lung Cancer Patients Using a Microcavity Array System," PLoS One, vol. 8, no. 6, p. e67466, Jun. 2013.
- [3] A. Das, C. Singha, and A. Bhattacharyya, "Development of silicon microneedle arrays with spontaneously generated micro-cavity ring for transdermal drug delivery," *Microelectron Eng*, vol. 210, pp. 14– 18, Apr. 2019.
- [4] M. Punjiya, A. Mocker, B. Napier, A. Zeeshan, M. Gutsche, and S. Sonkusale, "CMOS microcavity arrays for single-cell electroporation and lysis," *Biosens Bioelectron*, vol. 150, p. 111931, Feb. 2020.
- [5] K. Takahashi et al., "Circulating tumor cells detected with a microcavity array predict clinical outcome in hepatocellular carcinoma," Cancer Med, vol. 10, no. 7, pp. 2300–2309, Apr. 2021.
- [6] X. Han et al., "Advances in high-performance MEMS pressure sensors: design, fabrication, and packaging," Microsystems and Nanoengineering, vol. 9, no. 1. Springer Nature, Dec. 01, 2023.
- [7] H. Zhang, C. Zhang, J. Chen, and A. Li, "A Review of Symmetric Silicon MEMS Gyroscope Mode-Matching Technologies," *Micromachines*, vol. 13, no. 8. MDPI, Aug. 01, 2022.

- [8] W. Niu et al., "Summary of Research Status and Application of MEMS Accelerometers," *Journal of Computer and Communications*, vol. 06, no. 12, pp. 215–221, 2018.
- [9] Y. Gao, L. Yu, J. Chuan Yeo, and C. Teck Lim, "Flexible Hybrid Sensors for Health Monitoring: Materials and Mechanisms to Render Wearability," *Advanced Materials*, vol. 32, no. 15, p. 1902133, Apr. 2020.
- [10] H. Fallahi, J. Zhang, H. P. Phan, and N. T. Nguyen, "Flexible microfluidics: Fundamentals, recent developments, and applications," *Micromachines*, vol. 10, no. 12. MDPI AG, Dec. 01, 2010
- [11] A. Golparvar, S. Tonello, A. Meimandi, and S. Carrara, "Inkjet-Printed Soft Intelligent Medical Bracelet for Simultaneous Real-Time Sweat Potassium (K+), Sodium (Na+), and Skin Temperature Analysis," *IEEE Sens Lett*, vol. 7, no. 5, May 2023.
- [12] D. H. Choi, M. Gonzales, G. B. Kitchen, D. T. Phan, and P. C. Searson, "A Capacitive Sweat Rate Sensor for Continuous and Real-Time Monitoring of Sweat Loss," ACS Sens, vol. 5, no. 12, pp. 3821–3826, Dec. 2020.
- [13] D. Bejarano, P. Lozano, D. Mata, S. Cito, M. Constanti, and I. Katakis, "Screen printing as a holistic manufacturing method for multifunctional microsystems and microreactors." *J. Micromech. Microeng*, 19, 115007, Oct. 2009